6th Australasian Hydraulics and
Fluid Mechanics Conference
Adelaide, Australia, 5-9 December 1977

Incompressible Laminar and Turbulent Flow in the Entrance Region of a Smooth Circular Pipe

A. K. MOHANTY

Assistant Professor in Mechanical Engineering, Indian Institute of Technology, Kharagpur, India

and

S. B. L. ASTHANA

Research Scholar, Indian Institute of Technology, Kharagpur, India

SUMMARY Laminar and turbulent incompressible flow in the entrance region of a smooth pipe is analysed by dividing the region into two parts; inlet and filled. Experimental data corroborate the theoretical findings.

C_f Skin friction coefficient

$C_f = \frac{\tau_w}{1/2\rho U_{oo}^2}$; $C_{f_1} = \frac{\tau_w}{1/2\rho\ U_o^2}$

H shape parameter = $\frac{\delta^*}{\delta^{**}}$

n velocity profile index in turbulent flow

p static pressure; p_o, static pressure at inlet;

$p^* = \frac{p_o - p}{1/2\rho\ u_o^2}$

r radial coordinate; R, radius of the pipe

Re Reynolds number = $\frac{2U_o R}{\nu}$

u axial component of velocity; U_o, area average velocity

U_∞ free stream velocity; U_c, centre line velocity in the filled region

$\bar{u}$ non-dimensionalized axial velocity =

$\frac{u}{U_\infty}$ or $\frac{u}{U_c}$

v radial component of velocity

x axial coordinate; $x_1 = \frac{x}{R}$

x_e axial coordinate at the end of filled/entrance region

x_f axial coordinate at the end of inlet region

y vertical distance from the wall of the pipe

δ boundary layer thickness;

$\delta_1 = \frac{\delta}{R}$, $\delta_1 = 1$ in the filled region

δ^* displacement thickness =

$\int_o^\delta (1 - \frac{u}{U_\infty})(1 - \frac{y}{R})\,dy$; $\delta_1^* = \frac{\delta^*}{R}$

δ^{**} momentum thickness =

$\int_o^\delta \frac{u}{U_\infty}(1 - \frac{u}{U_\infty})(1 - \frac{y}{R})\,dy$; $\delta_1^{**} = \frac{\delta^{**}}{R}$

η non-dimensionalized wall distance = $\frac{y}{\delta}$

λ pressure gradient parameter =

$\frac{\delta^2}{\nu}\frac{dU_\infty}{dx}$ or $\frac{R^2}{\nu}\frac{dU_c}{dx}$; $\lambda_1 = \frac{6(\lambda - 2\ \delta_1)}{6 + \delta_1}$

Γ second pressure gradient parameter =

$\frac{R^2}{U_c}\left(\frac{\partial^2 u}{\partial y^2}\right)_{y=R}$; $\Gamma_1 = \frac{\Gamma}{6 + \delta_1}$

μ coefficient of dynamic viscosity

ν coefficient of kinematic viscosity

ρ density of the fluid

τ_w wall shear stress

ξ non-dimensionalized axial distance = $\frac{x}{R.Re}$

1 INTRODUCTION

Investigation of laminar incompressible fluid flow in the entrance region of a pipe, or a duct, has been reported by several workers. The physical model hitherto chosen consists of a viscous boundary layer near the wall and a potential core in the centre.

While Schlichting (1934) carried out a series solution for the potential core velocity; Schiller (1922), an integral analysis with second order velocity profile in the boundary layer; Atkinson and Goldstein (1938), an addition of velocity defect to the final fully developed Poiseuille solution; in all these analyses, the tacit assumption has been that the similar velocity profile of the fully developed flow is reached simultaneously at the location where the boundary layers meet at the pipe axis - consequenting on the vanishing of the potential core.

Experimental observations by the present authors however, indicate that the potential core vanished much earlier (inlet region) and that adjustment of a completely viscous profile (filled region) preceeds the attainment of fully developed flow. A passing reference to such a phenomenon was indicated by Goldstein (1938).

In carrying out the present analysis, the entrance region has therefore been assumed to consist of (i) an 'inlet region' with potential core where boundary layer equations are applicable, and (ii) a completely viscous 'filled region' where Navier-Stokes equation, with order of magnitude analysis, if possible, has to be applied.

Comparatively limited reference exists for the case of turbulent flow in the entrance region. Aside

from the elimination of the filled region, the analysis due to Ross and Whippany (1956) assumes that the laws of velocity profile and shear stress in the fully developed flow are applicable in the entrance region. Barbin and Jones (1963) assumed a 1/7th power law, but did not derive any law for wall shear stress in the entrance region. The fully developed and the entrance regions differ in the nature of pressure gradient, and Ross's assumptions or Barbin's profile are questionable.

In this paper, the laminar flow analyses are confirmed by experiments and generalised turbulent flow laws are derived by combining experimental and analytical informations.

2 ANALYSIS

2.1 Laminar Flow

The physical model of the flow in the entrance region, together with the chosen coordinate system is shown in Figure 1

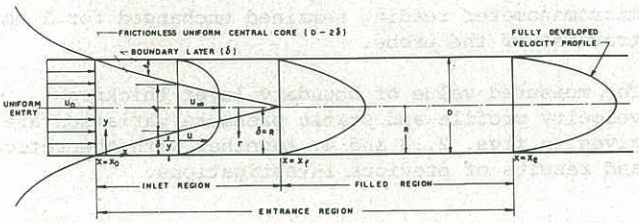

Figure 1 Physical model of entrance region

Incompressible, steady, axi-symmetric flow of a homogenous, isotropic fluid with uniform velocity at entrance tothe pipe is considered without viscous dissipation.

It is assumed that the length of the inlet region x_f, is large compared to boundary layer thickness and the length of the filled region is too large compared to the pipe radius.

2.1.1 Governing equations

Order of magnitude analysis using $\frac{R}{x_e - x_f}$

$<<1$, leads to $\frac{\partial^2 u}{\partial x^2} << \frac{1}{r}\frac{\partial}{\partial r}(r\frac{\partial u}{\partial r})$

in the filled region, and the resulting momentum equation has the form similar to boundary layer equation of the inlet region.

The governing equations for conservation of mass and momentum are

$$\frac{\partial}{\partial x}\left[(R-y)u\right] - \frac{\partial}{\partial y}\left[(R-y)v\right] = 0 \qquad (1)$$

$$u\frac{\partial u}{\partial x} - v\frac{\partial u}{\partial y} = -\frac{1}{\rho}\frac{dp}{dx} + \frac{\nu}{R-y}\frac{\partial}{\partial y}\left[(R-y)\frac{\partial u}{\partial y}\right] \qquad (2)$$

$0 \leq y \leq \delta$ in the inlet region

$0 \leq y \leq R$ in the filled region

The following boundary conditions are applied to choose a velocity profile for a Von-Karman-Pohlhausen type integral solution of the flow with pressure gradient in both the inlet and the filled region.

The boundary conditions are

$u = 0$, $v = 0$ at $y = 0$, no slip condition

$u = U_\infty$ or $u = U_c$ and

$\frac{\partial u}{\partial y} = \frac{\partial^2 u}{\partial y^2} = 0$ at $y = \delta$

Additionally, from momentum equation

$$\left(\frac{\partial^2 u}{\partial y^2}\right)_{y=0} - \frac{1}{R}\left(\frac{\partial u}{\partial y}\right)_{y=0} = -\frac{U_\infty}{\nu}\frac{dU_\infty}{dx} \quad \text{in the inlet region}$$

or $\left(\frac{\partial^2 u}{\partial y^2}\right)_{y=0} - \frac{1}{R}\left(\frac{\partial u}{\partial y}\right)_{y=0} = -\frac{U_c}{\nu}\frac{dU_c}{dx} + 2\left(\frac{\partial^2 u}{\partial y^2}\right)_{y=R}$

in the filled region

The velocity profile satisfying these boundary conditions are

$$\bar{u} = (2\eta - 2\eta^3 + \eta^4) + \frac{\lambda_1}{6}(\eta - 3\eta^2 + 3\eta^3 - \eta^4) - \frac{\Gamma_1}{2}(2\eta - 13\eta^2 + 20\eta^3 - 9\eta^4) \qquad (3)$$

for both the inlet and filled region while noting that $\Gamma_1 = 0$ in the inlet region. It would be noted that the velocity profile given by eq.(3) becomes parabolic of the fully developed flow, when $\lambda_1 = -\frac{12}{7}$ and $\Gamma_1 = -\frac{2}{7}$, resulting in $\bar{u} = 2\eta - \eta^2$. In other words the values of the pressure gradient parameters marking the end of the entrance region are

$$\lambda_1 = -\frac{12}{7} \text{ and } \Gamma_1 = -\frac{2}{7}.$$

2.1.2 Solution

The partial differential equations (1) and (2) of continuity and momentum are integrated between $\eta = 0$ to $\eta = 1$, to yield

$$\frac{d\,\delta_1^*}{d\xi} = \frac{1}{2}(1 - 2\,\delta_1^*)\frac{1}{U_c}\frac{dU_c}{d\xi} \qquad (4)$$

and $$\frac{d\,\delta_1^{**}}{d\,\xi} + \frac{\delta_1^{**}}{U_c}(H+2)\frac{dU_c}{d\xi} - \frac{2U_o\Gamma}{U_c} = \frac{C_f \cdot Re}{2}$$

$U_c \equiv U_\infty$ and $\Gamma_1 = 0$ in the inlet region (5)

The velocity profile defined by eq.(3) is used to evaluate the non-dimensional displacement and momentum thicknesses, δ_1^* and δ_1^{**}, and when substitution are made in eqs. (4) and (5), the following result

$$\frac{d\,\delta_1}{d\xi} = \frac{\delta_1 F_1 - \lambda_1 F_2}{\delta_1^2 F_3}\left(\frac{U_c}{U_\infty}\right) \qquad (6)$$

and

$$\frac{d\lambda_1}{d\xi} = \frac{\delta_1^4 F_4 \frac{d\delta_1}{d\,\xi} - F_5\left(\frac{U_o}{U_\infty}\right)^2}{F_6} \qquad (7)$$

in the inlet region

$$\frac{d\Gamma_1}{d\xi} = \frac{F_7}{F_8}\frac{U_o}{U_c} \qquad (8)$$

and

$$\frac{d\lambda_1}{d\xi} = -30(7\lambda_1 + 12)\left(\frac{U_o}{U_c}\right)^2 \frac{9}{2}\frac{d\Gamma_1}{d\xi} \qquad (9)$$

in the filled region,

where F_1 to F_6 are functions of $\lambda 1$ and δ_1, and F_7 and F_8 are functions of λ_1 and Γ_1, and are defined in the appendix.

The variation of δ_1 and λ_1 in the inlet region and Γ_1 and λ_1, in the filled region, respectively from sets of eqs. (6, 7) and (8,9) are obtained by numerical solution using Runge-Kutta method and the results are given in Figs. 2 and 3.

Knowledge of local values of δ_1, λ_1 and Γ_1 enables evaluation of velocity profile; from whence the skin friction coefficient using Newton's law of wall shear stress, and pressure gradient in the inlet region using Bernoulli's equation are evaluated.

Bernoulli's equation is not applicable in the filled region in the absence of a potential core; the pressure gradient here is evaluated numerically by Taylor's series expansion

$$\frac{p_o - p_{\xi+\Delta\xi}}{\frac{1}{2}\rho U_o^2} = \frac{p_o - p_\xi}{\frac{1}{2}\rho U_o^2} - \left(\frac{\partial p}{\partial \xi}\right)_{\text{at } \xi+\frac{\Delta\xi}{2}} \Delta\xi \qquad (10)$$

It is observed that the boundary layer thickness becomes equal to pipe radius, $\delta_1 = 1$, at $\xi = 0.036$ where $\lambda_1 = 2.727$. The end of the filled region, which also marks the end of the entrance region, was said to be reached when $U_{max}/U_o = 2$ (within a numerical deviation of less than 1%) at $\xi = 0.150$, where $\lambda_1 = -1.6830$ (ideal $\lambda_1 = -1.7143$) and $\Gamma_1 = -0.2839$ (ideal $\Gamma_1 = -0.2857$) were reached.

2.2 Turbulent Flow

An analysis for the turbulent flow in the entrance region could be carried out in a similar manner, if suitable laws for the velocity profile and the wall shear stress were known.

It would be observed from the experimental results reported in the succeeding section that a power law profile

$$\frac{u}{U_\infty} = \left(\frac{y}{\delta}\right)^{1/n}$$

with value of n dependent on Reynolds number, and a law of wall shear stress different from fully developed flow could be applied to the inlet portion of the entrance region.

On the basis of such laws, the various parameters are

$$\delta 1^* = \frac{\delta_1}{n+1} - \frac{\delta_1^2}{4n+2}$$

and

$$\delta_1^{**} = \frac{n}{(n+1)(n+2)}\delta_1 - \frac{n}{(2n+1)(2n+2)}\delta_1^2$$

The continuity and momentum equations yield respectively

$$\frac{U_o}{U_\infty} = 1 - 2\,\delta_1^*, \qquad (11)$$

$$\frac{d\,\delta_1}{dx_1} = \frac{n+2}{(n+1)(2n+1)} \frac{F_{10}^3}{F_9 F_{10} + F_{11} F_{12}} C_{f_1}, \qquad (12)$$

F_9 to F_{11} being defined as in the appendix. The velocities are their time-mean values.

From these two equations (11) and (12) numerical evaluation of δ_1 is possible, when the value of n and C_{f_1}, determined from experiments are substituted.

The values of δ_1 so evaluated are compared with experimental data in fig. 5.

3 EXPERIMENTS

3.1 Laminar Flow

Low velocity air flow corresponding to Reynolds numbers 1875, 2500 and 3250 was created through a 30 mm i.d. smooth aluminium pipe of 6 metres length from a large settling chamber; the connection between the pipe and the chamber being a smooth reentrant bell-mouth ensuring uniform velocity at entrance. Static pressure variation was measured along the length of the pipe. An impact micro-probe made out of 2mm i.d. hypodermic needle with flattened end was fitted to a micrometer for the total pressure traverse at different axial position. An Askania micromanometer with 0.01 mm wg. sensitivity was used for velocity head measurement. The potential core was said to be reached when the micromanometer reading remained unchanged for 1 mm traverse of the probe.

The measured value of boundary layer thickness, velocity profile and static pressure variation are given in figs. 2, 3 and 4, together with theoretical and results of previous investigations.

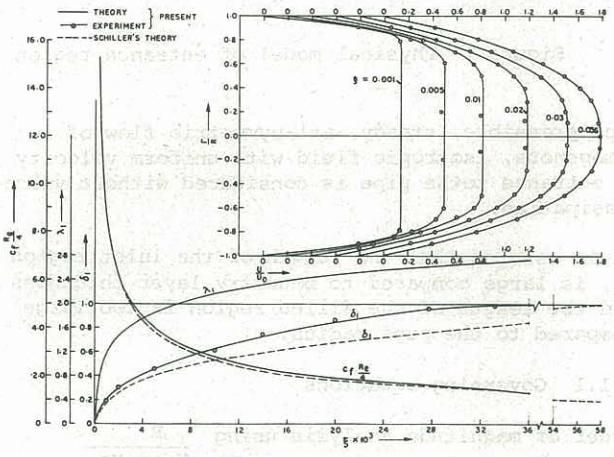

Figure 2 Flow parameters in the inlet region, laminar flow

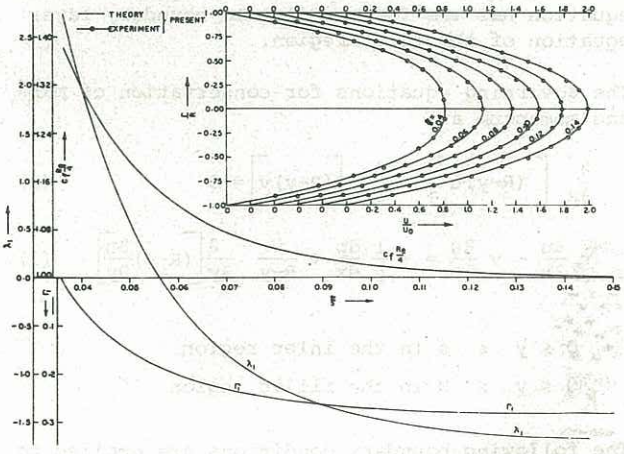

Figure 3 Flow parameters in the filled region, laminar flow

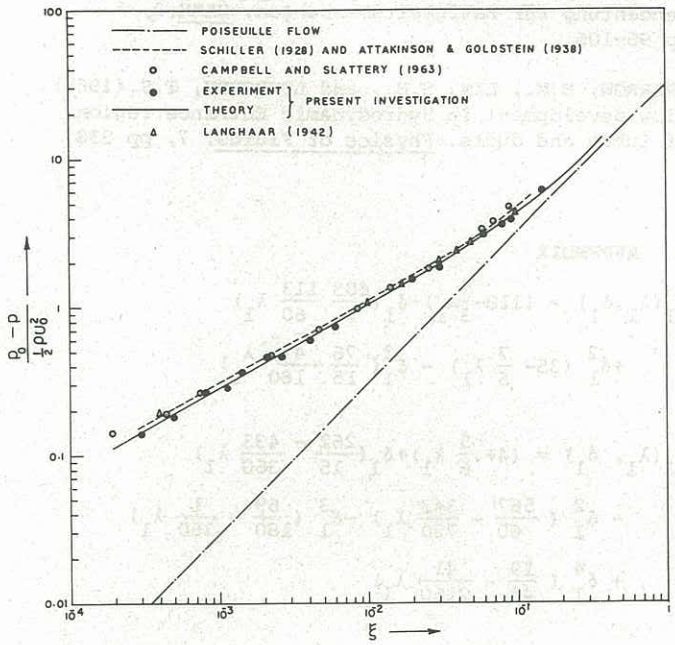

Figure 4 Pressure drop in the entrance region, laminar flow

3.2 Turbulent Flow

Similar measurements of static pressure variation boundary layer thickness and velocity profile were carried out in turbulent flow through a pipe of 40 mm i.d., 650mm in length at Reynolds numbers 66750 and 82250.

A summary of experimental data indicated that

n = 9.3 for Re = 66750 and n = 9.5 for Re= 82750

By a control volume analysis over small sections of the inlet region, it was possible to estimate discrete local value of wall shear stress that could be considered constant over the section under consideration, from the measured values of static pressure and computed values of momentum using the measured velocity profile.

A Blasius type correlation was undertaken to obtain an emperical relation for C_{f_1}, as

$$\frac{C_{f_1}}{2} = C_1 \left(\frac{U_\infty}{U_o}\right)^{\frac{2n}{n+1}} Re_\delta^{\frac{-2}{n+1}}$$

where $C_{f_1} = \frac{\tau_\omega}{\frac{1}{2}\rho U_o^2}$, $Re_\delta = \frac{U_o \delta}{\nu} = \frac{Re}{2}\delta_1$

From experiments $C_1 = A\, x_1^{-m}$, with
m = 0.001 and
A = 0.01305 for
Re = 66750
A = 0.0125 for
Re = 82250

As indicated in 2.2, these expressions for C_{f_1} and values for n for different Reynolds number are used to solve the conservation equations for δ_1, which in turn is compared with experiments.

4 CONCLUSIONS

In figs. 2,3, and 4, the results of analysis and experiments together with the results of earlier investigations for laminar flow are presented. The major conclusions are

(i) The inlet portion with a potential core exists till

$$\xi_f = \frac{x}{R.Re} = 0.036,$$ followed by the viscous filled region of $\xi_e - \xi_f = 0.114$ so that the total entrance length is $\xi_e = 0.15$. This value compares well with the results of Atkinson and Goldstein (1938) and Campbell and Slattery (1963) based on velocity defect analysis obtaining ξ_e = 0.13 and 0.136 respectively.

(ii) The calculated static pressure variation agrees well with the measurements of the present and earlier investigations.

(iii) The terminal values of λ_1 and Γ_1 differ from their exact values by less than 2%. The agreement of λ_1 and Γ_1 and the static pressure variation lays confidence to the present analysis based on the hypothesis of inlet and filled portions in the entrance region.

The results for turbulent flow are summarised as

(iv) Measurements indicate that the velocity profile in the inlet region has a Reynolds number dependent index different from fully developed value. It is plausible to hypothesize, on the basis of observations in the laminar flow, that this index undergoes adjustment in a filled region to finally attain the constant fully developed value.

(v) Both the boundary layer thickness and shear stress coefficients have been evaluated using suggestion of Ross and Whippanny (1956) and Ludwieg and Tillman (1949). Their relations which are same as/or derived for fully developed data, fail to verify either of the above two parameters; nor even the pressure gradient variation. On the other hand the present correlations derived independently from experiments when used in the conservation equations predict experimentally attainable boundary layer thickness, fig. 5, and static pressure variation, fig. 6.

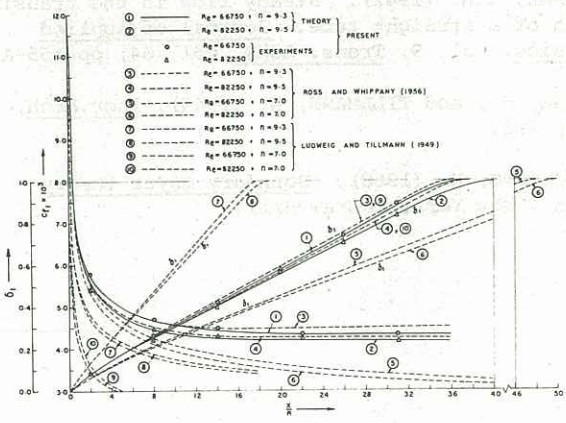

Figure 5 Boundary layer thickness and shear stress in the inlet region, turbulent flow

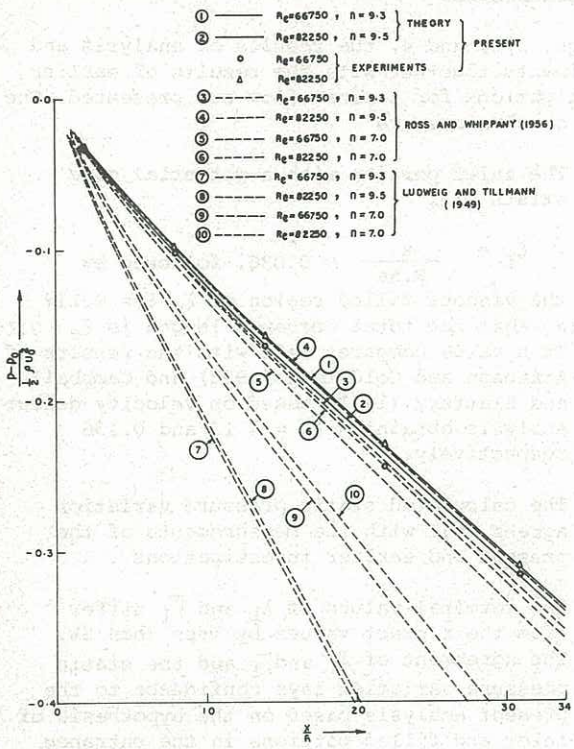

Figure 6 Pressure drop in the inlet region, turbulent flow

5 REFERENCES

BARBIN, A.R., and JONES, J.B. (1963). Turbulent flow in the inlet region of a smooth pipe. Journal of Basic Engg., Trans. ASME, Vol.85, Series D, pp 29-34.

BOWLUS, D.A., and BRIGHTON, J.A. (1968). Incompressible turbulent flow in the inlet region of a pipe. Journal of Basic Engg., Trans. ASME, September, pp 431-433.

CAMPBELL, W.D., and SLATTERY, J.C. (1963). Flow in the entrance region of a tube. Journal of Basic Engg., D.85, pp 41-46.

DONALD ROSS and WHIPPANY, N.J. (1956). Turbulent flow in the entrance region of a pipe. Transactions of ASME, vol. 78, pp 915-922.

GOLDSTEIN, S. (1938). Modern developments in fluid dynamics. vol. 1, England, Clarendon Press Oxford, pp

LANGHAAR, H.L. (1942). Steady flow in the transition length of a straight tube. Journal of Applied Mechanics, vol. 9, Trans. ASME, vol. 64, pp A55-A58

LUDWIEG, H., and TILLMANN, W. (1949). Ingr.Arch, 17, pp 288.

SCHLICHTING, H. (1968). Boundary layer theory 6th ed., New York, McGraw-Hill.

SCHILLER, L. (1922). Die Entwicklung der laminaren Geschwindigkeitsverteilung und ihr Bendentung für Zahigkeitsmessungen. ZAMM, 2, pp 96-106.

SPARROW, E.M., LIN, S.H., and LUNDGREN, T.S. (1964). Flow development in Hydrodynamic Entrance region of tubes and ducts. Physics of Fluids, 7, pp 338

6 APPENDIX

$$F_1(\lambda_1,\delta_1) = (118-\frac{5}{3}\lambda_1)-\delta_1(\frac{483}{5}\frac{113}{60}\lambda_1) +\delta_1^2\ (35-\frac{7}{5}\lambda_1) - \delta_1^3(\frac{76}{15}-\frac{41}{180}\lambda_1)$$

$$F_2(\lambda_1,\delta_1) = (4+\frac{5}{6}\lambda_1)+\delta_1(\frac{262}{15}-\frac{433}{360}\lambda_1) - \delta_1^2(\frac{567}{60}-\frac{343}{720}\lambda_1) -\delta_1^3(\frac{69}{180}-\frac{1}{360}\lambda_1) + \delta_1^4(\frac{19}{45}-\frac{41}{2160}\lambda_1)$$

$$F_3(\lambda_1,\delta_1) =(\frac{537}{200}-\frac{1}{4}\lambda_1+\frac{1}{288}\lambda_1^2) - \delta_1(2-\frac{5}{24}\lambda_1+\frac{1}{288}\lambda_1^2) + \delta_1^3(\frac{3}{10}-\frac{1}{30}\lambda_1+\frac{1}{1440}\lambda_1^2)$$

$$F_4(\lambda_1,\delta_1) = (108-3\lambda_1) - \delta_1(48-2\lambda_1)$$

$$F_5(\lambda_1,\delta_1) = 720\,\delta_1 + 360\,\lambda_1 + 60\,\lambda_1\,\delta_1$$

$$F_6(\lambda_1,\delta_1) = \delta_1^3\,(3-\delta_1)$$

$$F_7(\lambda_1,\Gamma_1) = -95040 + 22608\lambda_1 + 168\lambda_1^2 - 473904\,\Gamma_1 - 4248\lambda_1\,\Gamma_1 - 972\Gamma_1^2 + 21\lambda_1^2\,\Gamma_1 - 567\lambda_1\,\Gamma_1^2$$

$$F_8(\lambda_1,\Gamma_1) = 864-9\lambda_1 + 243\,\Gamma_1$$

$$F_9(\delta_1,n) = 2(n+1) - 2n(n+2)\,\delta_1$$

$$F_{10}(\delta_1,n) = (n+1)(2n+1)-2(2n+1)\delta_1+(n+1)\delta_1^2$$

$$F_{11}(\delta_1,n) = (4n+2) - (2n+2)\,\delta_1$$

$$F_{12}(\delta_1,n) = (4n+2)(3n+2)\delta_1 - (n+2)(3n+1)\delta_1^2$$